

AN ABSTRACT OF THE THESIS OF

Ziyan Liu for the degree of Master of Science in Chemical Engineering presented on December 3, 2018.

Title: Novel Interfacial Syntheses of Covalent Organic Frameworks

Abstract approved: _____

Chih-hung Chang

Covalent organic frameworks (COFs) are an emerging type of microporous crystalline polymers connected by organic units via strong covalent bonds. Due to the well-defined crystalline structure and excellent chemical and thermal stabilities, COF materials are being considered as promising candidates in a variety of applications, such as gas adsorption, catalysis and energy storage. Compared with metal-organic frameworks (MOFs), COFs exhibits lower density due to no existence of heavy metal elements. However, demanding synthesis requirements such as high temperature and long reaction time prevents the development of COFs synthesis in large scale.

In this thesis, interfacial polymerization which is operated under ambient condition is explored for the formation of COFs. COF-TAPB-TFP made from the condensation of 1,3,5-tris(4-aminophenyl) benzene (TAPB) and 1,3,5-triformylphloroglucinol (TFP) and COF-TAPB-TFB made from 1,3,5-tris(4-aminophenyl) benzene (TAPB) and 1,3,5-triformylbenzene (TFB) were firstly synthesized via the interfacial method. COF-TAPB-PDA that contains 1,3,5-tris(4-aminophenyl) benzene (TAPB) and terephthaldehyde (PDA) as building units was interfacial synthesized by using m-cresol as organic phase instead of aggressive 1,4-dioxane and mesitylene.

A novel strategy that utilize a sodium alginate layer to control the mass transfer was tested and resulted in COF membrane with improved quality.

X-ray diffraction (XRD), scanning electron microscope (SEM), Fourier transform infrared (FTIR) spectroscopy and the nitrogen sorption isotherm analysis were performed to characterize the various COFs synthesized from these experiments. These characterizations indicate successful formation of targeted COF membranes at the interfaces.

This work provides a facile and safe strategy to fabricate COFs membrane under ambient conditions. The free-standing membrane can be transferred onto other substrates to explore their potential applications in filtering large molecules in the future.

©Copyright by Ziyang Liu

December 3, 2018

All Rights Reserved

Novel Interfacial Syntheses of Covalent Organic Frameworks

by
Ziyan Liu

A THESIS

submitted to

Oregon State University

in partial fulfillment of
the requirements for the
degree of

Master of Science

Presented December 3, 2018
Commencement June 2019

Master of Science thesis of Ziyang Liu presented on December 3, 2018

APPROVED:

Major Professor, representing Chemical Engineering

Head of the School of Chemical, Biological, and Environmental Engineering

Dean of the Graduate School

I understand that my thesis will become part of the permanent collection of Oregon State University libraries. My signature below authorizes release of my thesis to any reader upon request.

Ziyang Liu, Author

ACKNOWLEDGEMENTS

I like to express my sincere gratitude and heartfelt appreciation to Dr. Chih-Hung Chang for accepting me into his research group. Also, I am deeply appreciative to Dr. Chang for his heuristic suggestion and inspirational encouragement through the experiment.

I would like to extend my appreciation to my committee members: Dr. Keith L. Levien, Dr. Zhenxing Feng, and Dr. Kaichang Li for their time and commitment to my MS defense presentation.

For the NMR measurement, I would like to thank NMR facility manager Stephen Huhn for his hard work to help me measure samples and provide a lot of advises.

For Electron Microscope images, I would like to thank our group members Yujing Zhang and Mei Han for their help without any complaints.

For Surface Areas Measurement, I would like to thank Dr. David Ji for the access of the BET instrument from his group and Dr. Zhifei Li for training me how to operate it.

Particularly, I want to thank Yujing Zhang for guiding me during the experiment and offering me useful suggestions when I am confused.

I also want to thank all of my group members Changqing Pan, Yujuan He, Zhongwei Gao, Yujing Zhang, Han Mei, Shujie Li, Ceng Zeng, Yu Cao, Hao Sun and Venkata Vinay for their academic assistance and all others who ever helped me.

Finally, I like to dedicate my most grateful blessing to my loving parents and family for their financial and spiritual support.

TABLE OF CONTENTS

	Page
1 Literature Review.....	1
1.1 Structures of COFs	1
1.2 Classification of COFs.....	2
1.2.1 Boron-containing COFs.....	2
1.2.2 Triazine-based COFs (CTFs).....	3
1.2.3 Imide-linked COFs	3
1.2.4 Imine-linked COFs	4
1.3 Synthesis methods	5
1.3.1 Solvothermal synthesis	6
1.3.2 Microwave synthesis.....	6
1.3.3 Ionothermal synthesis	7
1.3.4 Room- temperature synthesis.....	7
1.3.5 Liquid-liquid interfacial synthesis	8
1.4 Applications of COFs	10
1.4.1 Gas adsorption and sensing.....	10
1.4.2 Catalysis.....	10
1.4.3 Electric applications.....	11
1.5 References	11
2 Experiments	14
2.1 Materials	14
2.2 Solvothermal synthesis of COFs.....	14
2.2.1 Synthesis of 1,3,5-triformylphloroglucinol.....	14
2.2.2 Synthesis of COF-TpFn	16
2.2.3 Synthesis of TAPB-TFP	17
2.3 Doping iodine into COF-TpFn	17
2.4 Interfacial synthesis of TAPB-TFP and TAPB-TFB at room temperature	18
2.5 Interfacial synthesis of TAPB-PDA at room temperature	21
2.6 References	25
3 Results and Discussions.....	27
3.1 General methods	27
3.2 Characterization of COF-TpFn.....	27
3.3 Characterization of TAPB-TFP	31
3.4 Characterization of TAPB-TFB membrane	31
3.5 IV measurement of iodine doped COFs.....	32
3.6 Characterization of TAPB-PDA membrane	33
4. Conclusion and Future Works	37
4.1 Conclusion	37
4.2 Future work.....	37
Appendix: ¹ H and ¹³ C NMRs for Synthesized Compounds	38

LIST OF FIGURES

Figure	Page
Figure 1 Self-condensation of BDBA.....	2
Figure 2 Co-condensation of BDBA and HHTP	3
Figure 3 Cyclotrimerization of DCB	3
Figure 4 Condensation of PMDA and TAPA.....	4
Figure 5 (A) Condensation of “Schiff base” COFs; (B) Condensation of “hydrazine” COFs; (C) Condensation of “azine” COFs; (D) Condensation of “beta-ketonamine” COFs	5
Figure 6 Schematic of an interfacial polymerization reaction	9
Figure 7 Synthesis of 1,3,5- triformylphloroglucinol (TFP).....	15
Figure 8 Improved synthesis of 1,3,5- triformylphloroglucinol (TFP).....	16
Figure 9 (A) Synthesis of COF-TpFn; (B) Schematic representation of the solvothermal synthesis of TpFn.....	17
Figure 10 Solvothermal synthesis of TAPB-TFP	17
Figure 11 (A) Pictures of TpFn sample in each step; (B) picture of sample pellet	18
Figure 12 (A) Synthesis of TAPB-TFP; (B) Schematic representation of the interfacial synthesis of TAPB-TFP; (C) Picture of TAPB-TFP membrane	20
Figure 13 (A) Synthesis of TAPB-TFB; (B) Schematic representation of the interfacial synthesis of TAPB-TFB; (C) Picture of TAPB-TFB membrane	21
Figure 14 Schematic of interfacial synthesis procedure of TAPB-PDA	22
Figure 15 (A) Synthesis of TAPB-PDA; (B) Schematic representation of the interfacial synthesis of TAPB-PDA; (C) Picture of TAPB-PDA membrane	23
Figure 16 (A) Synthesis of TAPB-PDA by adding sodium alginate into the aqueous solution; (B) Picture of TAPB-PDA membrane	24
Figure 17 (A) The photo of Franz cell; (B) an oblique view of a jacketed Franz cell with a flat ground joint [1]	25
Figure 18 Photo of TAPB-PDA membrane synthesized in Franz cell	25

LIST OF FIGURES (Continued)

Figure	Page
Figure 19 PXRD pattern and structure of COF-TpFn	28
Figure 20 Infrared spectra of TpFn COF	29
Figure 21 PXRD of TpFn synthesized via improved solvothermal method (black solid); conventional solvothermal method (red dot); and water-based hydrothermal method (blue, dash)	29
Figure 22 N ₂ adsorption isotherms of TpFn synthesized using the improved solvothermal (black), the conventional (red) and water-based (blue) route.	30
Figure 23 (A) PXRD of TAPB-TFP powder (black) and film (red); (B) FTIR spectra of TAPB- TFP film (red) and powder (black)	31
Figure 24 (A) PXRD of TAPB-TFB film; (B) FTIR spectra of TAPB-TFB film (red) and powder (black)	32
Figure 25 Current-voltage measurement of COF-TpFn (A) and I ₂ @ TpFn (B)	33
Figure 26. Infrared spectra of TAPB-PDA membrane	33
Figure 27 PXRD patterns of TAPB-PDA films synthesized with sodium alginate (red) and without sodium alginate (black) and TAPB-PDA powder synthesized via solvothermal route (blue)	34
Figure 28 (A) SEM images of TAPB-PDA membrane at different magnifications and (B) photo of TAPB-PDA membrane	35
Figure 29 (A) SEM images of TAPB-PDA membrane synthesized by introducing sodium alginate in spacer layer and (B) photo of TAPB-PDA membrane	35
Figure 30 N ₂ adsorption isotherms of TAPB-P	36

LIST OF TABLES

Table	Page
Table 1 Density, d , and viscosity, η , data for sodium alginate aqueous solutions at $T = 298.15$ K and at atmospheric pressure	24
Table 2 Surface areas of TpFn synthesized via different methods	30

1 Literature Review

Covalent organic frameworks (COFs) are a class of emerging microporous crystalline materials consisting of light elements (such as H, B, C, N, and O) which form two-dimensional (2D) and three-dimensional (3D) structures via strong covalent bonds. The first COFs material is designed and synthesized by Dr. Yaghi and co-workers in 2005 [1]. Heretofore multifarious COFs have been designed and synthesized as potential materials with multiple applications such as gas adsorption and storage, catalysts and energy storage. In this thesis, some basic concepts including the structure, mechanism, synthesis and applications will be reviewed based on the recent development of COFs. The thesis work mainly focuses on the interfacial synthesis of COFs materials at room temperature.

1.1 Structures of COFs

For polymeric materials synthesis, irreversible process always leads to amorphous structure, while reversible reactions usually activate the structure into well-defined crystalline due to the conversion of bonds during the reaction. Stable covalent bonds are formed via varied synthetic organic reactions between the building blocks, which provide the COFs with reticular chemistry periodic structure. The structure of COFs is determined by the geometry of the organic ligands. Therefore, two prerequisites must be concerned for synthesizing crystalline COFs: (1) the reaction is under the reversible condition and (2) the appropriate building blocks (organic ligands) to constitute the robust structure. [3]

By linked with diverse building blocks, COFs can be classed into either two-dimensional (2D) or three-dimensional (3D) framework. For 2D COFs, the organic ligands are assembled on 2D planes which then stack by layers to form a layered eclipsed structure. This high-ordered structure could improve charge carrier mobility in the stack direction. Thus, the 2D COFs usually present good potential in fluorescence and photovoltaics applications. Compared with 2D structure, the 3D COFs are extended on three-dimensional space by the existence of sp^3 carbon or silane atom. Therefore, this type of structure gives unique characters such as high surface

areas, many open sites in the framework, and low densities, which make 3D COFs ideal for molecular capture or gas storage.

1.2 Classification of COFs

1.2.1 Boron-containing COFs

Several reaction mechanisms have been explored for the COFs materials. The first examples of COFs, developed by Yaghi and co-workers, is based on the boronate ester linkage of boronic acid. Boronic acid blocks also can be connected with dialcohols to form COFs via the formation of boronate ester or boronate. One strategy to form the boron-containing COFs is via the self-condensation of boronic acid building blocks such as the COF-1, synthesized via the self-condensation of 1,4-benzenediboronic acid (BDBA). [1]

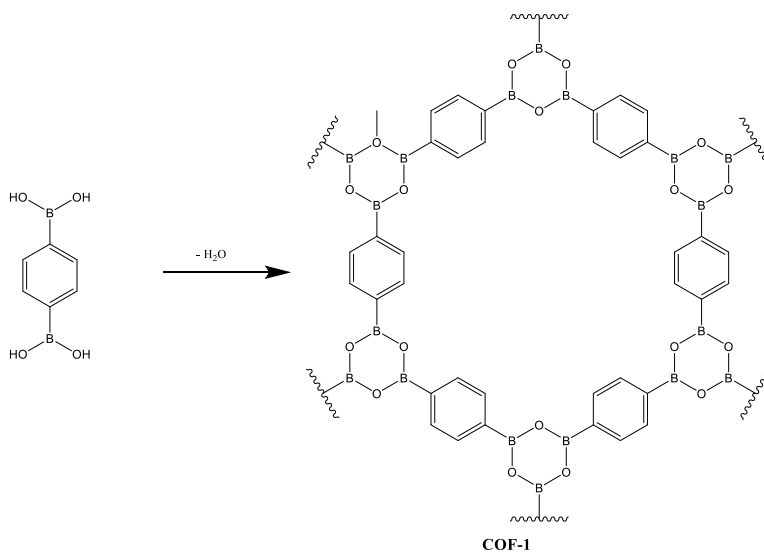


Figure 1 Self-condensation of BDBA

The other strategy of boron-containing COFs is the co-condensation of two or more different organic ligands. A range of COFs via the co-condensation have been prepared by choosing different building blocks. The most typical COF researched by Yaghi and the co-workers is COF-5 which is synthesized by 1,4-benzenediboronic acid (BDBA) and hexahydroxytriphenylene (HHTP).

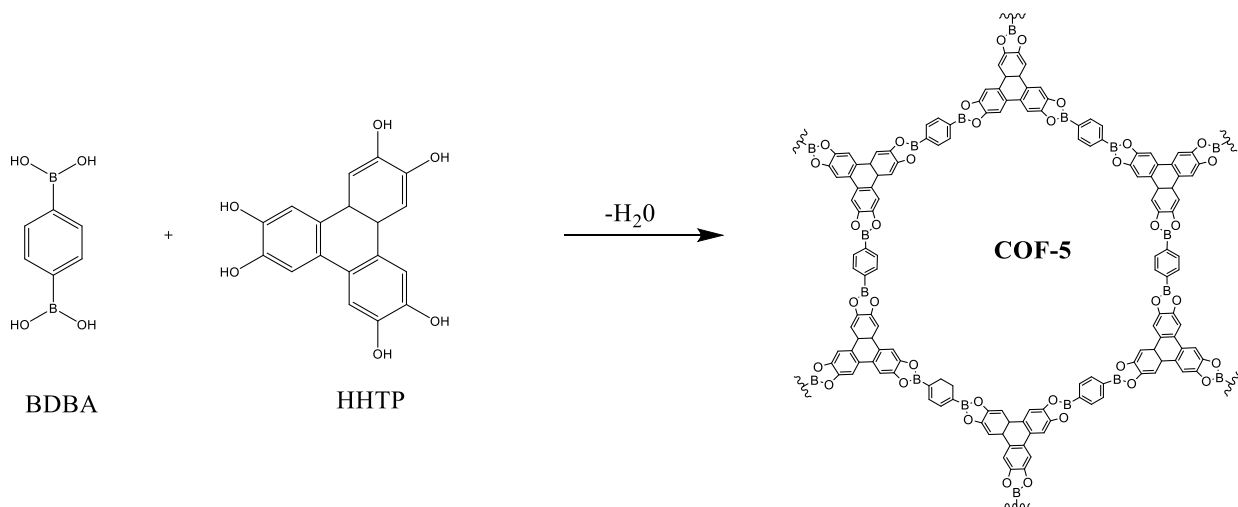


Figure 2 Co-condensation of BDBA and HHTP

1.2.2 Triazine-based COFs (CTFs)

The second mechanism for COF is triazine-based COFs (CTFs). The first CTF was made by Thomas and co-workers via the cyclotrimerization of nitrile monomer 1,4-dicyanobenzene (DCB) [4]. Even though the low crystallinity leads to the CTFs poor reversibility, the CTFs have attracted tremendous attention for diverse applications such as photocatalysis [5], supercapacitor [6] and chemical sensing [7] due to the rich nitrogen content and excellent chemical stability.

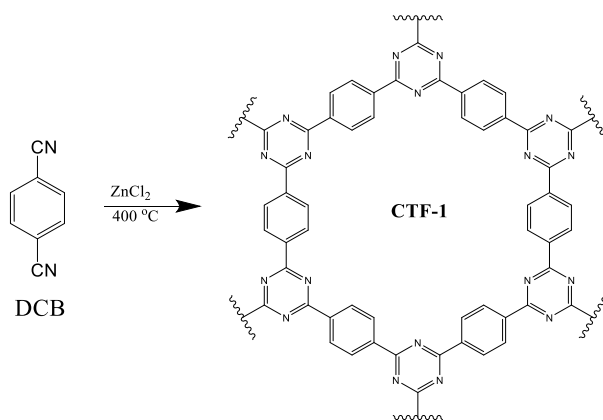


Figure 3 Cyclotrimerization of DCB

1.2.3 Imide-linked COFs

The third type of COFs is based on the imide formation reaction. The first imide-linked COFs were prepared by Yan and co-workers in 2014 [8]. These types of COFs have high surface area and excellent thermal stability which have promising applications for loading dye molecules and drug delivery [9]. The typical imide-linked COF, PI-COF-1, is synthesized by the condensation of pyromellitic dianhydride (PMDA) and triamine tris (4-aminophenyl) amine (TAPA).

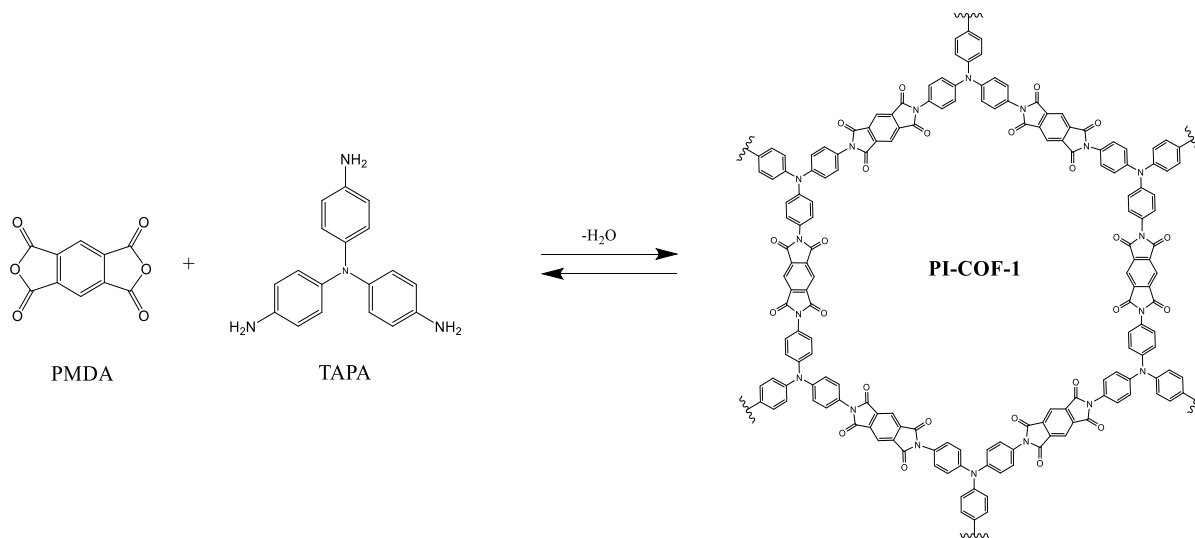


Figure 4 Condensation of PMDA and TAPA

1.2.4 Imine-linked COFs

Another class of COFs is based on the imine-based reaction. In 2009, Yaghi and co-workers discovered the first COF (COF-300) which is synthesized by tetra-(4-aminyl) methane (TAM) and terephthalaldehyde (PDA) via the imine-linkage [10]. Basically, these type of COFs can be categorized into four groups based on the formation of linkages: (1) Schiff base COFs are based on the condensation of aldehydes monomers and amines ones via the Schiff base reaction; (2) hydrazine COFs are based on the condensation reaction of aldehydes and hydrazides, called “hydrazine” reaction. Imine-linkage COFs; (3) azine COFs are based on the condensation of hydrazine and aldehyde to form hydrazine linkage; (4) the first step to form beta-ketonamine COFs is “Schiff-base” reaction. Then an irreversible enol-keto tautomerization is undergone to form a ketoenamine linkage. The formed ketoenamine COFs feature higher chemical stability due to the irreversible enol-keto tautomerization which prevents the deformation of linkage.

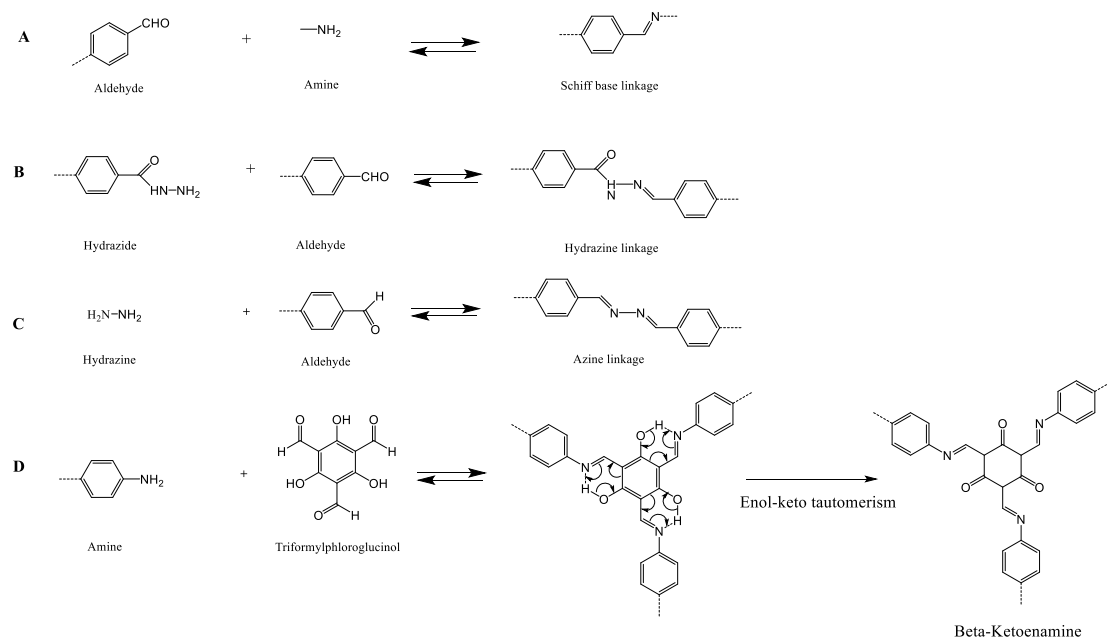


Figure 5 (A) Condensation of “Schiff base” COFs; (B) Condensation of “hydrazine” COFs; (C) Condensation of “azine” COFs; (D) Condensation of “beta-ketoenamine” COFs

Generally, imine-linked COFs present the following features: (1) a range of experimental conditions including room temperature reactions can be prepared; (2) a good many of precursors have been successfully used as condensation monomers including the 3-dimension one; (3) the COFs can be processed and deposited on substrates; (4) compared with boron-containing COFs, imine-linked COFs exhibit enhanced chemical and thermal stability due to the strong imine bond; (5) the imine-linked COFs have displayed a lot of properties and potential applications such as gas storage and catalysis.

1.3 Synthesis methods

Since the COFs can be designed via carefully choosing monomers and synthetic routes, synthetic conditions such as temperature, pressure, reaction time and the presence of catalyst are other important issue that should be considered for the COFs synthesis. Chemically stable, excellent porosity, and high crystallinity COFs can be synthesized by adopting the appropriate synthetic condition. Also, the suitable synthesis method will significantly reduce the reaction time and increase the product yield. Over the past decade, lots of reaction methods have been exploited for

the synthesizing COFs. Generally, the preparation methods of COFs can be summarized into the following methods: solvothermal, microwave, ionothermal synthesis and room-temperature synthesis.

1.3.1 Solvothermal synthesis

Solvothermal or hydrothermal synthesis is the main method to synthesize COFs and most of COFs are obtained via this method. The general route for the solvothermal method is following: (1) monomers dissolved in solvents are placed in a Pyrex tube or autoclave; (2) the solution or suspension are required to be degassed via freeze–pump–thaw cycles for several times to make sure no gas is in the system; (3) to provide isolated condition for the reaction, the tube has to be sealed by flame and heated to a designated temperature for a certain reaction time; (4) the product, usually as precipitate in the container, is collected, washed with suitable solvents, and dried under vacuum to yield the COF as solid powder. Issues such as the solubility, reaction rate, crystal nucleation, crystal growth rate, and ‘self-healing’ structure are important points to consider when selecting the reaction media and conditions.

Usually the reaction is placed in a hermetic container for three days or longer time and requires high temperature (70 - 120°C). In addition, the solvent needs to be degassed to remove any impurity to make higher quality products. Therefore, the demanding requests become high barriers for beginners to explore the reaction of COFs synthesis.

1.3.2 Microwave synthesis

Microwave-assisted heating is a highly efficient way to increase temperature quickly, which has been widely used for rapid and large-scale synthesis reaction for decades [2]. The first COF synthesized by microwave-assisted method was developed by Cooper and co-workers in 2009 [11]. Compared with the solvothermal synthesis, microwave-assist heating exhibits the following several strengths. (1) The reaction time of synthesizing COFs can be reduced significantly, which makes large-scale synthesis possible for industrial production. (2) The preparation for the solvothermal synthesis such as freeze–pump–thaw degassing and flaming-sealed vessel are not

required for the microwave method. (3) Microwave is a highly efficient way to heat and results in considerable energy saving. (4) Microwave-assisted heating is more eco-friendly than conventional heating ways. Also, microwave-assisted solvothermal reduces the usage of solvents. In conclusion, microwave heating provides a new possibility for further applications on industrialization, presenting a more efficient and cleaner methods for COFs.

1.3.3 Ionothermal synthesis

Ionothermal synthesis is the method utilizing ionic liquids as both the solvent and potential template to prepare crystalline material or grow single crystals. The first COFs synthesized via ionothermal method was explored by Thomas and co-workers in 2007 [12]. The ionic liquid, molten ZnCl_2 at 400°C , acts as functional solvent to catalyze the cyclotrimerization of aromatic nitrile building units (1,4-dicyanobenzene) and the covalent triazine-based frameworks (CTFs) are obtained with high crystallinity and stability. However, the high reaction temperature limits the scope of monomers for COFs synthesis. Hitherto, only few COFs can be synthesized by this method.

1.3.4 Room- temperature synthesis

In early research, the reactions of COFs were required to be done under high temperature to promote the condensation of monomers. Research on facilely synthesizing COFs at room temperature and ambient atmosphere is considered as promising potential topic for large-scale COFs production. Generally, mechanochemical grinding and rapid solution-phase synthesis have been explored as two approaches for room temperature synthesis of COFs.

Mechanochemical grinding has attracted growing attention as a facile method to synthesize COFs due to its fast process and environmentally friendly reaction condition compared with conventional solution-based synthesis such as solvothermal and microwave synthesis. Biswal et al. first synthesized beta-ketonamine COFs TpPa-1, TpPa-2 and TpBD via simply grinding precursors in mortar for approximately one hour [13]. While mechanochemical synthesis has lots

of strengths, the poor crystallinity and the porosity of mechanochemically synthesized COFs become arduous challenges for further research.

In 2015, Zamora and co-workers successfully synthesized RT-COF-1 (made from TAPB and TFB) by utilizing microfluidic system [14]. The COF obtained under continuous flow conditions exhibited excellent crystallinity and chemical stability. Almost at the same time, Yang et al. [15] fabricated COF-TpBD (made from TFP and benzidine (BD)) via simple and facile solution-phase synthesis at room-temperature. Shortly after, Zhao's group adopted the continuous flow system to synthesize COF-LZU-1 with higher crystallinity and porosity compared with the same kind of COF by traditional solvothermal method [16]. Moreover, the microfluidic synthesis of LZU-1 is claimed to possess a production rate of 41 mg per hour at an extremely high space-time yield of 703 kg m⁻³ per day, which exhibits favorable potential for large-scale synthesis of COFs. Later, in 2017, Dichtel and co-workers synthesized the imine-linked COFs TAPB-PDA, TAPB-BPDA and TAPB-TIDA in as little as 10 minutes at room-temperature by employing metal triflates to superiorly catalyze the formation of COF [17]. Not only the reaction temperature is optimized to ambient and the reaction duration is very short, the products obtained show outstanding porous structure with much higher BET surface area (2175 m² g⁻¹) in comparison with that via the traditional solvothermal synthesis. Even though these cases exhibit promising direction for the development of COFs synthesis, only few COFs have been demonstrated to be synthesized via the rapid solution-phase method. Solvothermal synthesis is still the most extensive method for COFs.

1.3.5 Liquid-liquid interfacial synthesis

Recently, interfacial polymerization has been proposed as another facile method to synthesize COFs membrane at room temperature due to its easy operation and safe reaction condition.

Interfacial polymerization is a favorable technique to produce membrane in large scale. It has been widely used to prepare defect-free, free-standing films of polymers and organic-inorganic hybrids. In an interfacial reaction system, there are two phases which are immiscible with each other to form the interface. Fig. 6 shows a schematic of an interfacial polymerization reaction.

Each phase contains a reaction monomer or catalyst. The reaction happens at the interface of two immiscible solvents. Since the polymerization is confined to the interface, the product is more inclined to form a uniform membrane instead of powder precipitation.

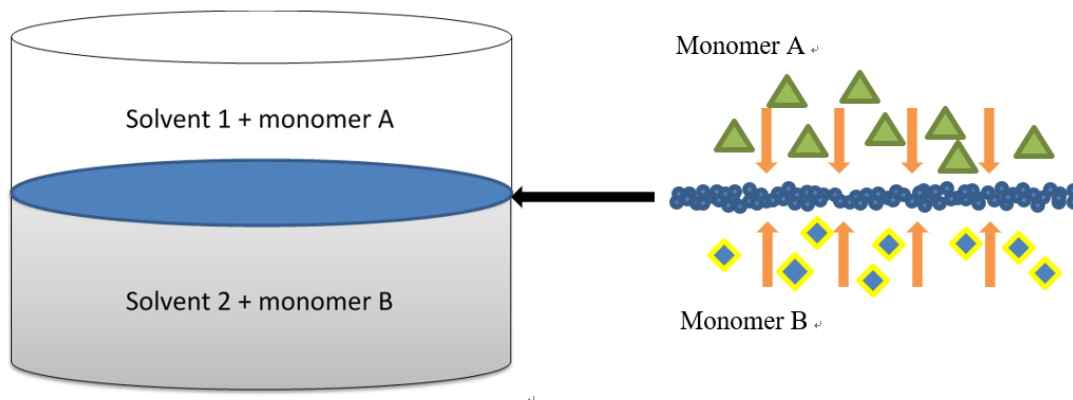


Figure 6 Schematic of an interfacial polymerization reaction

Banerjee and co-workers developed a strategy to synthesize keto-enamine COFs membranes via the interfacial method [18]. In this experiment, water dissolving amino monomer and dichloromethane dissolving aldehyde were chosen as two immiscible solvents. COFs are polymerized and transformed into membrane at the interface at room temperature. Dichtel and co-workers independently explored another interfacial method by using 1,4-dioxane, mesitylene as organic phase to synthesize TAPB-PDA thin film [19].

Liquid-liquid interfacial polymerization is a versatile synthetic strategy to fabricate COF thin films which possess appreciable performance. However, the research is still in nascence and many obstacles require to be overcome for the efficient product. Firstly, solvents used in the interfacial synthesis are corrosive such as 1,4-dioxane and dichloromethane, which confines the application on polymeric substrates including polyethersulfone (PES) and polysulfone (PSF) because corrosive solvents can corrode these polymers easily. What is more, compared with other facile synthesis such as mechanochemical method, interfacial synthesis usually requires long time to complete the reaction, typically several days, which constrains the potential for continuous manufacturing.

1.4 Applications of COFs

Similar with other porous materials such as metal-organic frameworks (MOFs), zeolitic imidazolate frameworks (ZIFs) and porous carbons, COFs have also been considered as potential candidates for further applications such as gas adsorption, catalysis and electric properties because of their high surface areas and crystalline structure. What is more, since COFs consist of light elements (such as H, B, C, N, and O) via strong covalent bonds, they present higher thermal and chemical stabilities compared with other organic-inorganic hybrids.

1.4.1 Gas adsorption and sensing

The storage of COFs for gases have been widely investigated including the adsorption of hydrogen, methane, and carbon dioxide [20]. However, the interaction between gas molecules and COFs is weak so that the intrinsic surface area plays a critical role in determining the capability of gas storage. 3D COFs present obviously higher uptake capacities than 2D COFs due to their larger surface area. For example, 3D COF-102, which has a BET surface area of $3620 \text{ m}^2\text{g}^{-1}$, is observed to have the gas uptake of 72 mg g^{-1} for H_2 , 187 mg g^{-1} for CH_4 , and 1180 mg g^{-1} for CO_2 [20]. Moreover, Murugavel and co-workers demonstrated that some COFs including TAPB-TFP, iPrTAPB-TFPB, iPrTAPB-TFP and TAPB-TFBP, exhibit fluorescence quenching when absorbing nitroaromatic gas, and thus these COFs exhibit potential with fluorescence and fluorescence chemo-sensing ability for nitroaromatic analytes [21].

1.4.2 Catalysis

COFs have promising potential in catalysis due to the porous structure and high stability. Wang and co-workers explored a Pd(II)-containing COF, Pd/COF-LZU1 which exhibits outstanding catalytic activity in catalyzing the Suzuki–Miyaura coupling reaction [22]. Another typical example is TPB-DMTP-COF, developed by the group of Jiang [23] in 2015, which can be applied in the field of organocatalysis.

1.4.3 Electric applications

The rigid backbone of two-dimension COFs can be shaped into hexagonal or tetragonal sheets to undergird the layer structure and the out-of-plane π interactions are salient in this stacking layers structure. Such a structure leads to a large electronic coupling between the π -orbitals of the stacking layers, which promotes the transport of charge carriers. Dichtel and co-workers reported that the 2D COF, DAAQ-TFP thin films could be applied for electrical energy storage (EES) devices [23]. Moreover, FL-COF-1 was demonstrated as promising thermoelectric material by doping iodine [24]. The iodine doped FL-COF-1 exhibited a high Seebeck coefficient of 2450 $\mu\text{V K}^{-1}$ and power factor of 0.063 $\mu\text{W m}^{-1} \text{K}^{-2}$ at room temperature.

In conclusion, COF materials exhibit diverse potential applications due to their porous and ordered structure. Other promising applications such as contaminant filtering and drug delivery are under research.

1.5 References

- [1] Cote, Adrien P., et al. "Porous, crystalline, covalent organic frameworks." *science* 310.5751 (2005): 1166-1170.
- [2] de la Hoz, Antonio, Angel Diaz-Ortiz, and Andres Moreno. "Microwaves in organic synthesis. Thermal and non-thermal microwave effects." *Chemical Society Reviews* 34.2 (2005): 164-178.
- [3] Feng, Xiao, Xuesong Ding, and Donglin Jiang. "Covalent organic frameworks." *Chemical Society Reviews* 41.18 (2012): 6010-6022.
- [4] Kuhn, Pierre, Markus Antonietti, and Arne Thomas. "Porous, covalent triazine - based frameworks prepared by ionothermal synthesis." *Angewandte chemie international edition* 47.18 (2008): 3450-3453.
- [5] Liu, Manying, et al. "Crystalline Covalent Triazine Frameworks by In Situ Oxidation of Alcohols to Aldehyde Monomers." *Angewandte Chemie* 130.37 (2018): 12144-12148.

- [6] Kim, Minjae, et al. "High performance carbon supercapacitor electrodes derived from a triazine-based covalent organic polymer with regular porosity." *Electrochimica Acta* 284 (2018): 98-107.
- [7] Das, Prasenjit, and Sanjay K. Mandal. "A dual-functionalized, luminescent and highly crystalline covalent organic framework: molecular decoding strategies for VOCs and ultrafast TNP sensing." *Journal of Materials Chemistry A* 6.33 (2018): 16246-16256.
- [8] Fang, Qianrong, et al. "Designed synthesis of large-pore crystalline polyimide covalent organic frameworks." *Nature communications* 5 (2014): 4503.
- [9] Fang, Qianrong, et al. "3D porous crystalline polyimide covalent organic frameworks for drug delivery." *Journal of the American chemical society* 137.26 (2015): 8352-8355.
- [10] Uribe-Romo, Fernando J., et al. "A crystalline imine-linked 3-D porous covalent organic framework." *Journal of the American Chemical Society* 131.13 (2009): 4570-4571.
- [11] Campbell, Neil L., et al. "Rapid microwave synthesis and purification of porous covalent organic frameworks." *Chemistry of Materials* 21.2 (2009): 204-206.
- [12] Kuhn, Pierre, Markus Antonietti, and Arne Thomas. "Porous, covalent triazine - based frameworks prepared by ionothermal synthesis." *Angewandte chemie international edition* 47.18 (2008): 3450-3453.
- [13] Biswal, Bishnu P., et al. "Mechanochemical synthesis of chemically stable isorecticular covalent organic frameworks." *Journal of the American Chemical Society* 135.14 (2013): 5328-5331.
- [14] de la Peña Ruigómez, Alejandro, et al. "Direct On - Surface Patterning of a Crystalline Laminar Covalent Organic Framework Synthesized at Room Temperature." *Chemistry—A European Journal* 21.30 (2015): 10666-10670.
- [15] Yang, Cheng-Xiong, et al. "Facile room-temperature solution-phase synthesis of a spherical covalent organic framework for high-resolution chromatographic separation." *Chemical communications* 51.61 (2015): 12254-12257.
- [16] Peng, Yongwu, et al. "Room temperature batch and continuous flow synthesis of water-stable covalent organic frameworks (COFs)." *Chemistry of Materials* 28.14 (2016): 5095-5101.
- [17] M. Matsumoto, R. R. Dasari, W. Ji, C. H. Feriante, T. C. Parker, S. R. Marder and W. R. Dichtel, *J. Am. Chem. Soc.*, 2017, 139, 4999–5002

- [18] Dey K, Pal M, Rout K C, et al. *Journal of the American Chemical Society*, 2017, 139(37): 13083-13091.
- [19] Matsumoto, Michio, et al. "Rapid, low temperature formation of imine-linked covalent organic frameworks catalyzed by metal triflates." *Journal of the American Chemical Society* 139.14 (2017): 4999-5002.
- [20] Furukawa, Hiroyasu, and Omar M. Yaghi. "Storage of hydrogen, methane, and carbon dioxide in highly porous covalent organic frameworks for clean energy applications." *Journal of the American Chemical Society* 131.25 (2009): 8875-8883.
- [21] Kaleeswaran, D., Pratap Vishnoi, and Ramaswamy Murugavel. "[3+ 3] Imine and β -ketoenamine tethered fluorescent covalent-organic frameworks for CO₂ uptake and nitroaromatic sensing." *Journal of Materials Chemistry C* 3.27 (2015): 7159-7171.
- [22] Ding, San-Yuan, et al. "Construction of covalent organic framework for catalysis: Pd/COF-LZU1 in Suzuki–Miyaura coupling reaction." *Journal of the American Chemical Society* 133.49 (2011): 19816-19822.
- [23] Mulzer, Catherine R., et al. "Superior charge storage and power density of a conducting polymer-modified covalent organic framework." *ACS central science* 2.9 (2016): 667-673.
- [24] Wang, Liangying, et al. "Fluorene-Based Two-Dimensional Covalent Organic Framework with Thermoelectric Properties through Doping." *ACS applied materials & interfaces* 9.8 (2017): 7108-7114.

2 Experiments

2.1 Materials

Unless stated otherwise all reagents were purchased from commercial sources and used without further purification. All reactions were performed under an air atmosphere, unless stated otherwise. Hexamethylenetetramine (99%), formamidine acetate (FA, >98%), phloroglucinol (>99%), m-cresol (>98%), dimethylacetamide (DMAC, \geq 99%), 1,4-dioxane (\geq 99%), mesitylene (\geq 99%), 1,2-dichlorobenzene (o-DCB, 99%), Scandium(III) triflate ($\text{Sc}(\text{OTf})_3$, >99%) and p-Toluenesulfonic acid monohydrate (PTSA, \geq 98.5%) was purchased from Sigma-Aldrich. Terephthalaldehyde (PDA, >98.0%), iodine (I_2 , >98.0%) and 2,7-diaminofluorene (DAFL, >98.0%) was purchased from TCI AMERICA. 1,3,5-tris(4-aminophenyl) benzene (TAPB, >98.0%), 1,3,5-benzenetricarbaldehyde (TFB, >98%) and 1,3,5-triformylphloroglucinol (TFP, >98%) was purchased from HongKong UCHEM Co., Ltd.

2.2 Solvothermal synthesis of COFs

2.2.1 Synthesis of 1,3,5-triformylphloroglucinol

1,3,5-triformylphloroglucinol (TFP) is a kind of formylate phenol monomer specifically used for beta-ketonamine COFs synthesis. TFP was synthesized following previously reported recipes [1-2].

30 mL trifluoroacetic acid was added into hexamethylenetetraamine (5.09 g, 36 mmol) and dried phloroglucinol (2.05 g, 16 mmol) under the protection of N_2 atmosphere. The solution was heated at 100 °C for ca. 3 hours. Then 50 mL of 3 M HCl was added and heated the solution at 100 °C for 1 hour. After cooling to room temperature, the solution was filtered through Celite, extracted with ca. 150mL dichloromethane three times, dried over magnesium sulfate, and filtered. Rotary evaporation of the solution afforded off-white powder with less than 10% yield.

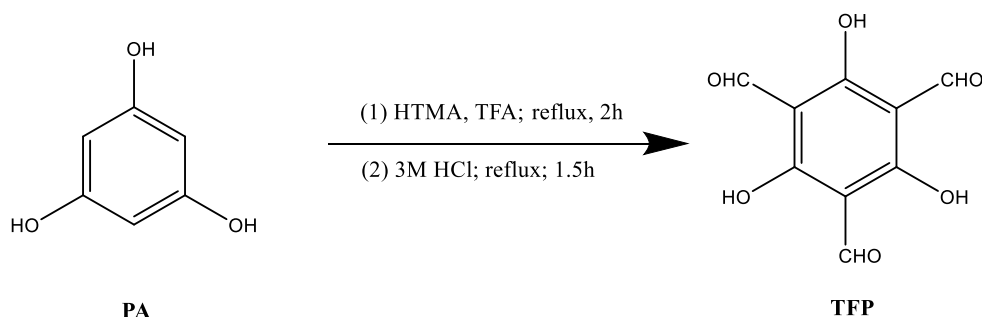


Figure 7 Synthesis of 1,3,5- triformylphloroglucinol (TFP)

Even though TFP can be synthesized by this procedure, the yield in the experiment is much lower than that in the reference (21%). Hence, the improved preparation developed by MacLachlan and co-workers [2] was operated to produce TFP for higher yield.

FA (4.12 g, 39.7 mmol, 2.5 equiv) and phloroglucinol (1.00 g, 8.0 mmol, 0.5 equiv) were mixed and dissolved in 100ml tetrahydrofuran (THF) in a round-bottom flask, stirring and heating to 45 °C. At this point acetic anhydride (7.35 mL, 80mmol, 5.0 equiv) was added, the flask was subsequently capped, and the reaction allowed to proceed for 24 hours. Then THF solvent and leftover acetic anhydride and acetic acid were evaporated under reduced pressure at 50 °C, followed by stirring in water (100 mL) at 40 °C for 2 hours. Aqueous LiOH (2 M, 300 mL, 600 mmol, 38 eq) was added slowly, then stirring continued for 18 hours. Aqueous hydrochloric acid (2 M, 150 mL, 300 mmol, 18.8 equiv) was added next to re-acidify the solution, causing a very pale salmon-colored powder to precipitate. The product was extracted into dichloromethane (4 × 30 mL), which was dried over magnesium sulfate and evaporated to give product TFP as an off-white powder with approximately 25 % yield. The product needed to be purified with column chromatography to remove impurities.

^1H NMR (800 MHz, DMSO) δ 9.98 (s, 3H; CHO), 5.75 ppm (s, 3H; OH), 3.95 ppm (s, 2H; H₂O). ^{13}C NMR (100 MHz, DMSO) δ 192 (CHO), 174.1 (COH), 103.2 ppm (CCHO). IR 1638, 1595, 1432, 1374, 1253, 1190, 1105, 968, 871, 808, 782, 600, 540 cm^{-1} .

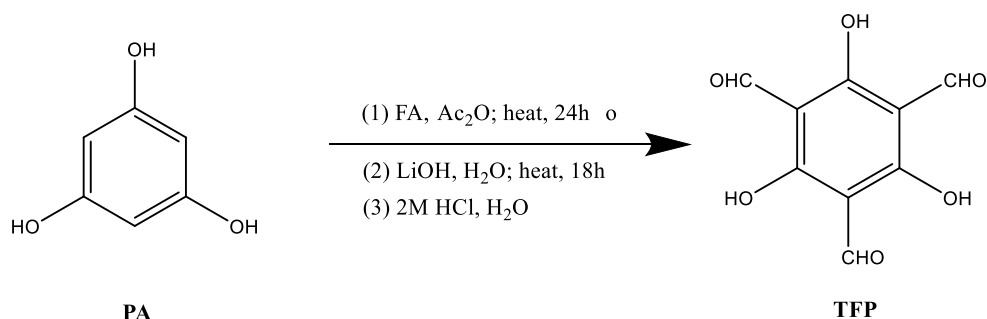


Figure 8 Improved synthesis of 1,3,5- triformylphloroglucinol (TFP)

2.2.2 Synthesis of COF-TpFn

COF-TpFn was designed and synthesized by the group of Banerjee in 2016 [3]. They used water to substitute aggressive and dangerous organic solvents such as dioxane and dichloromethane to synthesize COFs in water via dynamic covalent bonding. Despite the fact that it provides a viable, greener route to produce beta-ketoenamine COFs, the product synthesized via the water-based hydrothermal method showed worse crystallinity and lower surface area than that synthesized via the conventional solvothermal method. In the experiment, the conventional solvothermal synthesis was revised to improve the quality of product.

DAFL (124 mg, 0.64 mmol) and TFP (88 mg, 0.42 mmol) are suspended in 3 ml 1,2-Dichlorobenzene (o-DCB) and 3ml DMAC with 3 M acetic acid (1 mL) in a 30 ml three-neck round bottom flask. To degas the suspension, a balloon filled with nitrogen is connected to the flask by a three-way glass flow control adapter, and another joint is connected to vacuum. Firstly, close the joint between the balloon and adapter and open the vacuum to absorb air in the flask. Then close the joint connected to the vacuum and open the port between balloon and flask to make nitrogen fill in the reactor. Cycle the degassing procedure three times to replace the original gas in the flask with nitrogen. The flask is heated to 150 °C and reacted for 3 days with vigorous stirring. A red precipitate is obtained, which is collected by filtration. After being washed with THF and acetone three times, the deep red powder is dried in vacuum at 120 °C for 12 hours to afford COF-TpFn of 85 mg (87% yield).

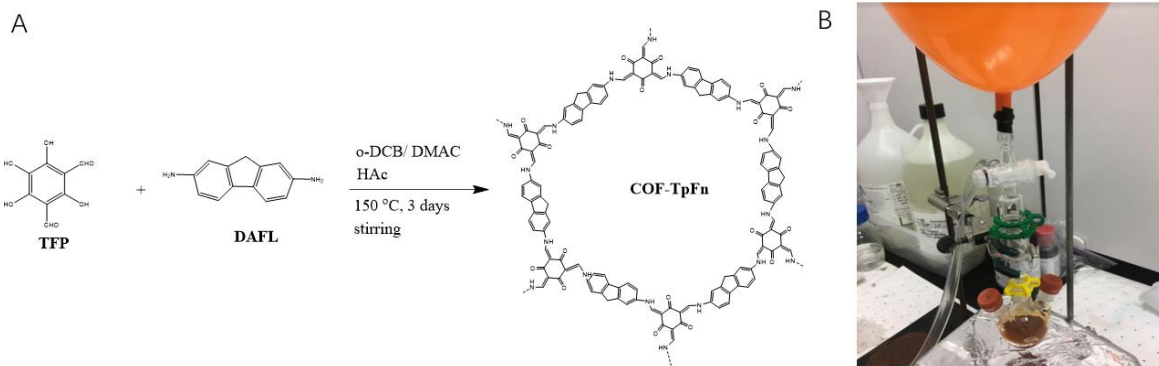


Figure 9 (A) Synthesis of COF-TpFn; (B) Schematic representation of the solvothermal synthesis of TpFn

2.2.3 Synthesis of TAPB-TFP

The synthesis of TAPB-TFP is followed by the procedure developed by Kaleeswaran et al. [4] A mixture of TAPB (100 mg, 0.284 mmol), TFP (60 mg, 0.28 mmol), 6 M aq. acetic acid (0.3 mL) and dry 1,4-dioxane (3 mL) was placed in a capped tube. The mixture was sonicated for 10 min to get a clear suspension. The capped tube then was heated at 110 °C for 5 days yielding an orange precipitate. The precipitate was isolated by filtration and washed with acetone, THF and then dried under high vacuum for 7 hours at 120 °C to afford TAPB-TFP (58 mg, 40%).

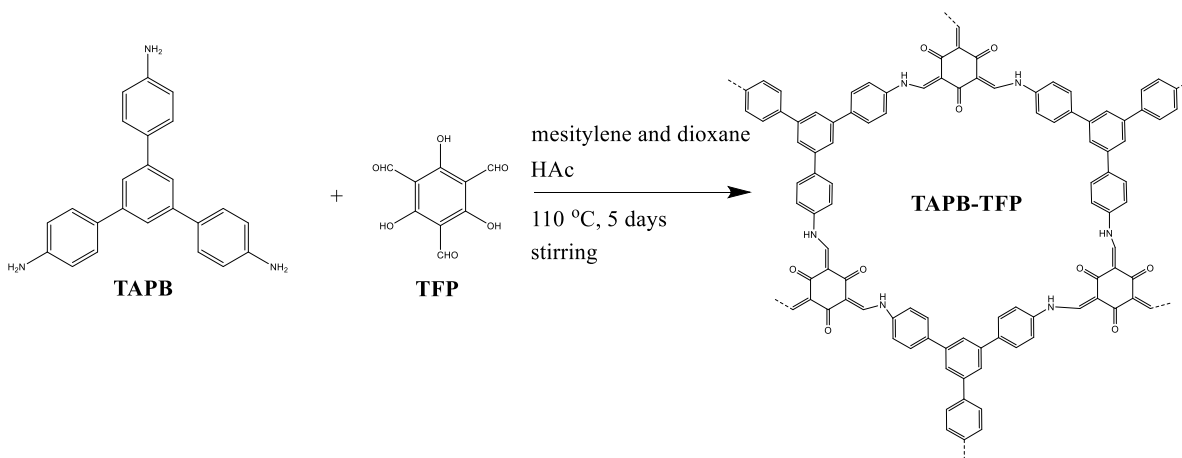


Figure 10 Solvothermal synthesis of TAPB-TFP

2.3 Doping iodine into COF-TpFn

Fluorene-based conjugated polymers have been considered as promising organic semiconductors because of their sterling electronic charge-transport properties. Wang and co-workers [5]

synthesized a kind of fluorene-based COF (FL-COF-1) via the polycondensation of DAFL and TFB. The FL-COF-1 exhibits excellent thermal stability (up to 460 °C) and high porosity structure with a BET surface area over 1300 m²g⁻¹ by introducing fluorene monomers into the frameworks. What is more, the presence of a π -conjugated backbone is proved that the charge carrier mobility can be increased significantly by doping with iodine. Similarly, the keto-type COF TpFn, bearing fluorene units in the amine ligands, is expected to present the enhanced charge carrier mobility via doping with iodine.

To prepare the iodine doped COF-TpFn, a small vial (5 mL) filled with 30 mg of the TpFn powder was placed into a brown vial (30 mL) charged with 500 mg of iodine, which was then capped tightly and kept in an oven at 75 °C for over 1 day. 95 mg iodine-adsorbed TpFn was obtained then heated at 75 °C under vacuum to remove any undoped iodine on the surface of the sample. After about 12 hours heating, the sample was observed to have no obvious weight change. Finally, 57.4 mg I₂@TpFn with deep brown color powder was gained. The sample was compressed into a circular pellet with 8 mm diameter and about 0.5 mm thickness for the further measurement.

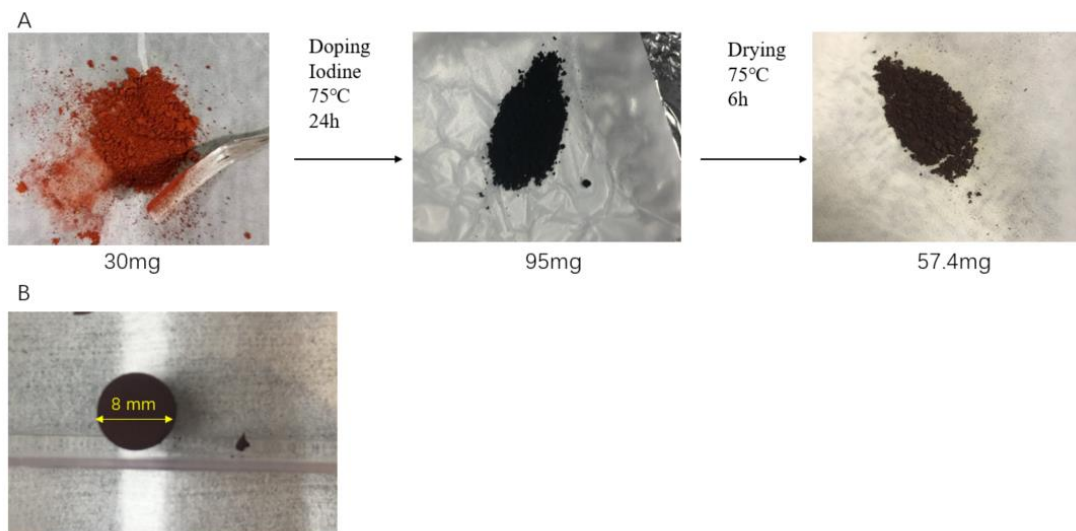


Figure 11 (A) Pictures of TpFn sample in each step; (B) picture of sample pellet

2.4 Interfacial synthesis of TAPB-TFP and TAPB-TFB at room temperature

The experiments on liquid-liquid interfacial synthesis of COFs is inspired by the work of Dey et al [6]. In the experiment, chloroform is the organic phase to pair with aqueous solution. As chloroform and water are immiscible with each other, a liquid-liquid interface can be created at the junction of these two solvents. Moreover, a salt-mediated technique [amine-p-toluene sulfonic acid (PTSA) salt] was employed as catalyst for the Schiff base reaction. The diffusion rate can be slowed down under the work of the H bonding within the PTSA-amine salt. As a result, a moderated reaction of precursors is carried out with the slower diffusion rate of the precursors through the interface to drive the reaction from the formation of amorphous polymers towards the thermodynamically controlled crystallization.

First, 100 ml of chloroform dissolved with TFP (16 mg, 0.076 mmol) was prepared and poured into a 400 ml beaker. Then 60 ml water was added as a space layer on top of the aldehyde solution. A mixture of TAPB (26 mg, 0.112 mmol) and PTSA salt (38.5 mg, 0.224 mmol) were dissolved in 70 mL of water and 30 mL of acetonitrile and added on top of the spacer solution through a peristaltic pump over a period of 30 minutes. The reaction system was placed at ambient temperature without any disturbance for 3 days. A piece of yellow membrane formed at the interface was collected, washed with water and acetone and then dried under vacuum. Finally, 3.9 mg of TAPB-TFP membrane was obtained with 8 % yield.

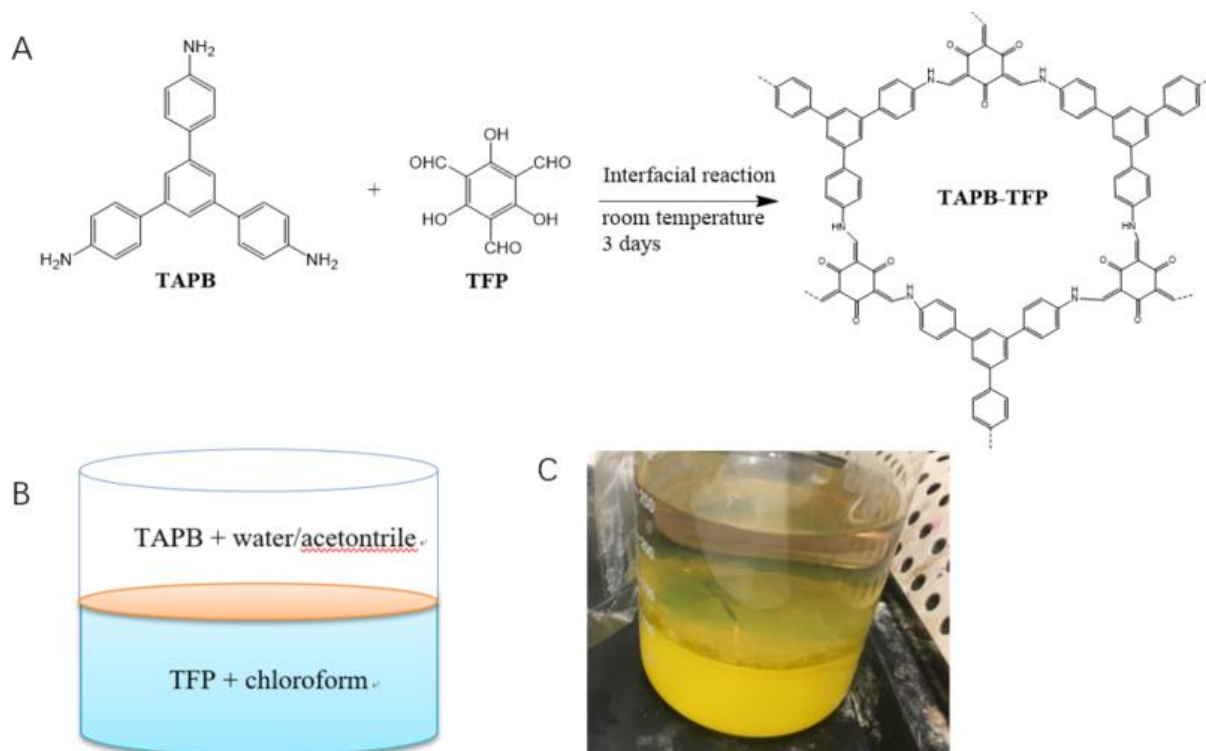


Figure 12 (A) Synthesis of TAPB-TFP; (B) Schematic representation of the interfacial synthesis of TAPB-TFP; (C) Picture of TAPB-TFP membrane

Puigmarti-Luis and co-workers confirmed that the reaction between TAPB and TFB in acetic acid under continuous microfluidic flow conditions at room temperature resulted in the formation of covalent organic framework [10]. As a result, TAPB-TFB can be synthesized under ambient conditions rapidly. Directly mixing TAPB and TFB in acetic acid at room temperature leads to jelly-like product which is washed with acetone to get yellow powder. To explore the fabrication of TAPB-TFB membrane, a procedure which is similar with the interfacial synthesis of TAPB-TFP was operated. Unlike the powder TAPB-TFB obtained by solvothermal method, the as-synthesized TAPB-TFB membrane is white in color.

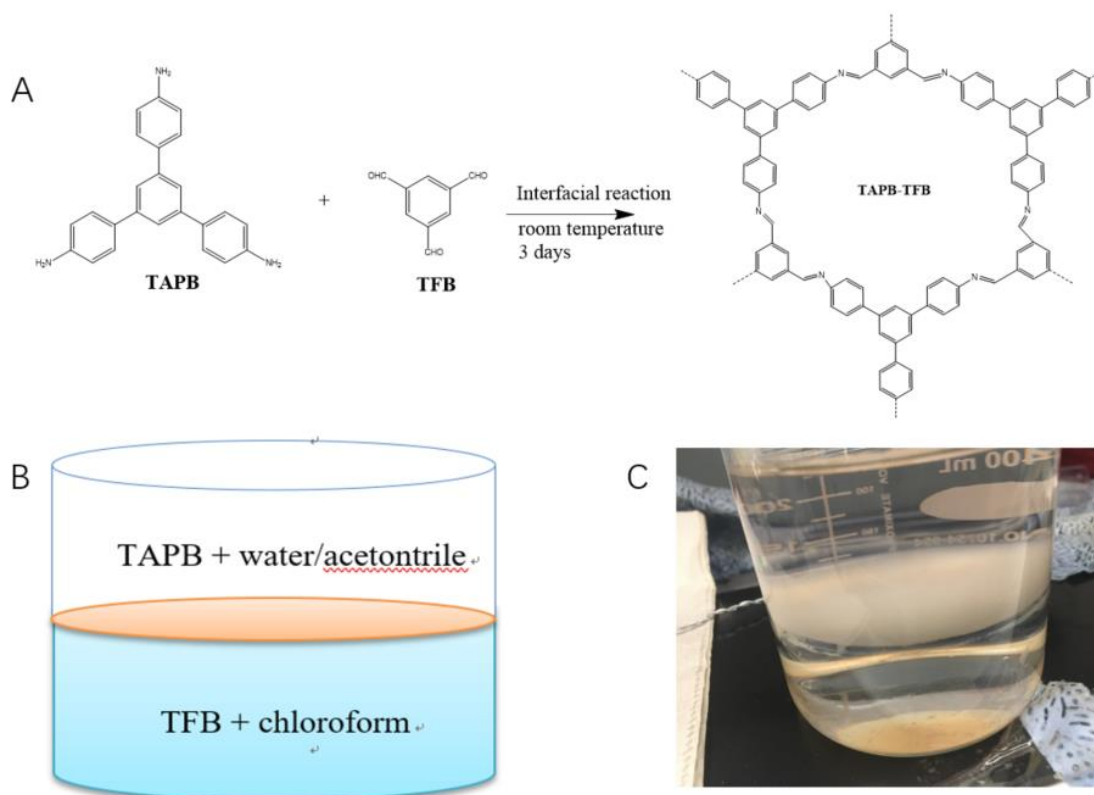


Figure 13 (A) Synthesis of TAPB-TFB; (B) Schematic representation of the interfacial synthesis of TAPB-TFB; (C) Picture of TAPB-TFB membrane

2.5 Interfacial synthesis of TAPB-PDA at room temperature

M-cresol which is immiscible with water was chosen as organic solution for the interfacial synthesis of TAPB-PDA. 36 mg TAPB dissolved in 10ml m-cresol was poured into a vial. 20mg PDA and 10mg of metal triflates $\text{Sc}(\text{OTf})_3$ dissolved in the aqueous solution (7ml water and 3ml acetonitrile) was layered on top of an organic solution. The system was kept at room temperature. The interface between organic and aqueous phase was observed as a curved surface instead of a plane. One of the reasons is that the density of m-cresol is close to that of water ($\rho_{\text{m-cresol}}$: 1.03 g/cm^3 STP), which makes the interface unstable as acetonitrile ($\rho_{\text{acetonitrile}}$: 0.786 g/cm^3 STP) diffusing into the organic solution. What is more, the area provided by the vial is too small to hold an interface. Organic-aqueous interface shaped into organic-aqueous-organic phase gradually, and two liquid-liquid interfaces were formed in the reaction system. After one day of reaction, yellow precipitate formed at top organic phases. The system was allowed to stay still for 72 hours in undisturbed condition. Yellow powder was collected and washed by ethanol over

three times to remove unreacted precursors and solvents residue adsorbed on the surface of COFs.

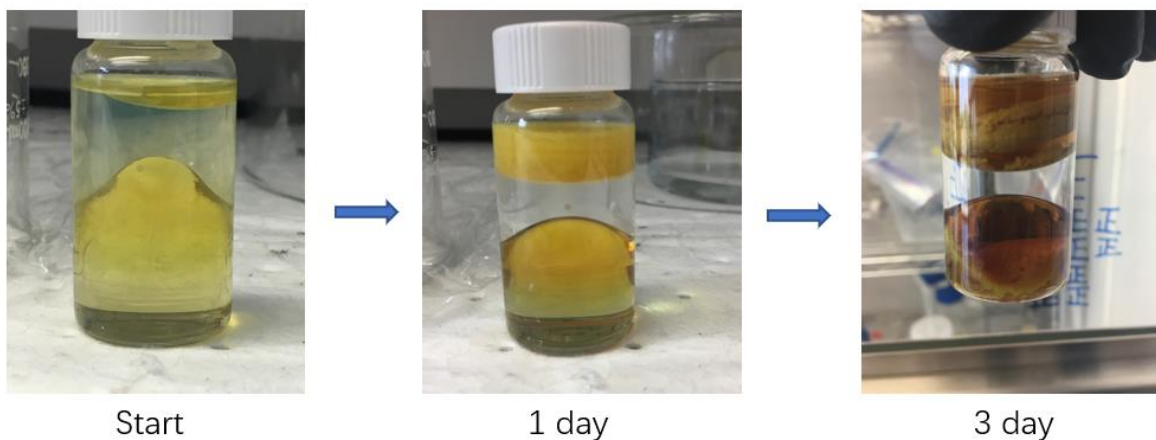


Figure 14 Schematic of interfacial synthesis procedure of TAPB-PDA

To revise the experiment, reducing the concentration of monomers and changing the container were attempted. First, 36 mg TAPB dissolved in 20mL of m-cresol was poured into the beaker. A spacer layer of 10 mL of water was added on top of the organic solution. 20 mg PDA- 4 mg Sc(OTf)₃ were dissolved in 15ml of water and 5 mL of acetonitrile and added slowly on top of the spacer solution over a period of 30 min. The system was kept at room temperature for 72 hours in undisturbed condition. Finally, yellow membrane was formed and washed by ethanol to remove impurities.

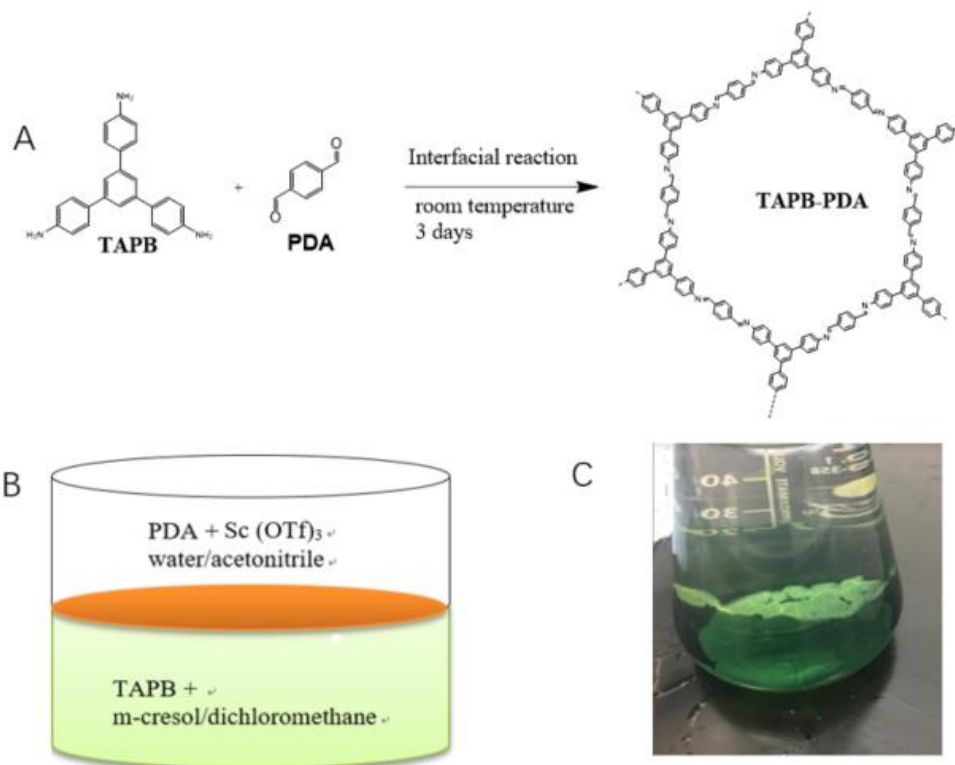


Figure 15 (A) Synthesis of TAPB-PDA; (B) Schematic representation of the interfacial synthesis of TAPB-PDA; (C) Picture of TAPB-PDA membrane

An improved method was tried to obtain more uniform membrane. As shown in Table 1, sodium alginate dissolved in water can increase the viscosity of solutions. As a result, sodium alginate is introduced into the spacer layer to slow down the diffusion rate of amino monomer in the aqueous phase. The slower diffusion rate of the precursors can promote the membrane grown at the interface to be more uniform and smooth. 45 mg 1,3,5-tris(4-aminophenyl) benzene (TAPB) dissolved in organic solution (16mL of m-cresol and 4ml dichloromethane) was poured into the beaker. A spacer layer of 10 mL of sodium alginate solution (0.25g/L) was added on top of the organic solution. Terephthalaldehyde (25mg)- Sc(OTf)₃ (15mg) were dissolved in 7ml of sodium alginate solution (0.25g/L) and 3 mL of acetonitrile and added slowly on top of the spacer solution. The reaction system was kept at room temperature without any disturbance for 3 days. A white color membrane shown in Fig 16 B was obtained at the interface and washed with ethanol to remove purities and afforded yellow transparent membrane.

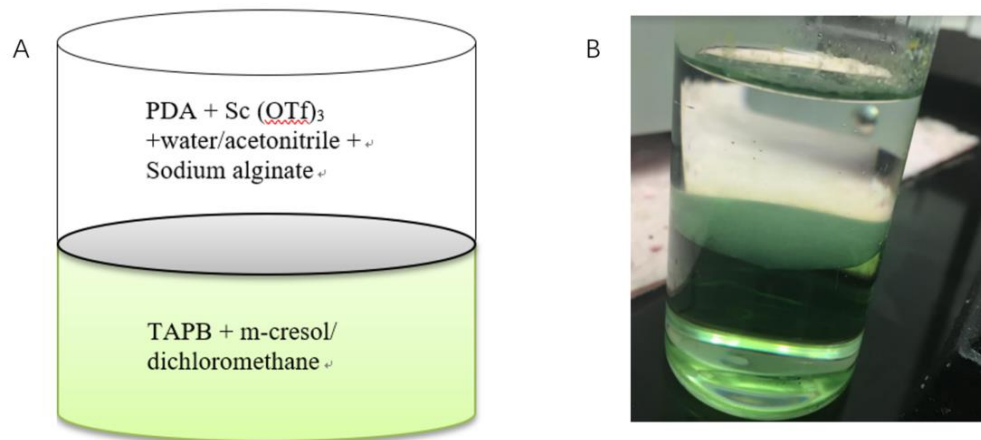


Figure 16 (A) Synthesis of TAPB-PDA by adding sodium alginate into the aqueous solution; (B) Picture of TAPB-PDA membrane

Table 1 Density, d , and viscosity, η , data for sodium alginate aqueous solutions at $T = 298.15$ K and at atmospheric pressure

$c/(g \cdot L^{-1})$	$d/(g \cdot cm^{-3})$	$\eta/(10^{-3} Pa \cdot s)$
0.00100c	0.99706	0.903
0.00500c	0.9971	0.921
0.01396	0.997106	0.914
0.10667	0.997144	1.337
0.26713	0.99722	2.034
0.5073	0.99734	2.706
1.01678	0.997681	4.037
4.9859	0.999809	13.74
7.49026	1.001365	37.54
9.98762	1.002704	70.14

Besides the using of sodium alginate to slow down the diffusion of monomer, another method is to introduce the interfacial reaction into the diffusion cell which can control diffusion. Franz cell is a kind of diffusion cell made of two individual glass components: the upper part called donor chamber and the lower part called receptor chamber [1]. The membrane which is used to slow down the diffusion is placed in the middle of the joint and held in place with a clamp.

Polypropylene membrane (Whatman, $0.2 \mu m$ pore size) and normal filter paper (Whatman, $11 \mu m$ pore size) were used as the membrane. One problem is that solution at upper chamber is very

difficult to diffuse into the receptor chamber due to the small pore size of the polypropylene membrane. When the filter paper is used in the Franz cell, the control of diffusion is not significant. Therefore, the COF synthesized in the Franz cell is not a smooth membrane shown in Fig 18.

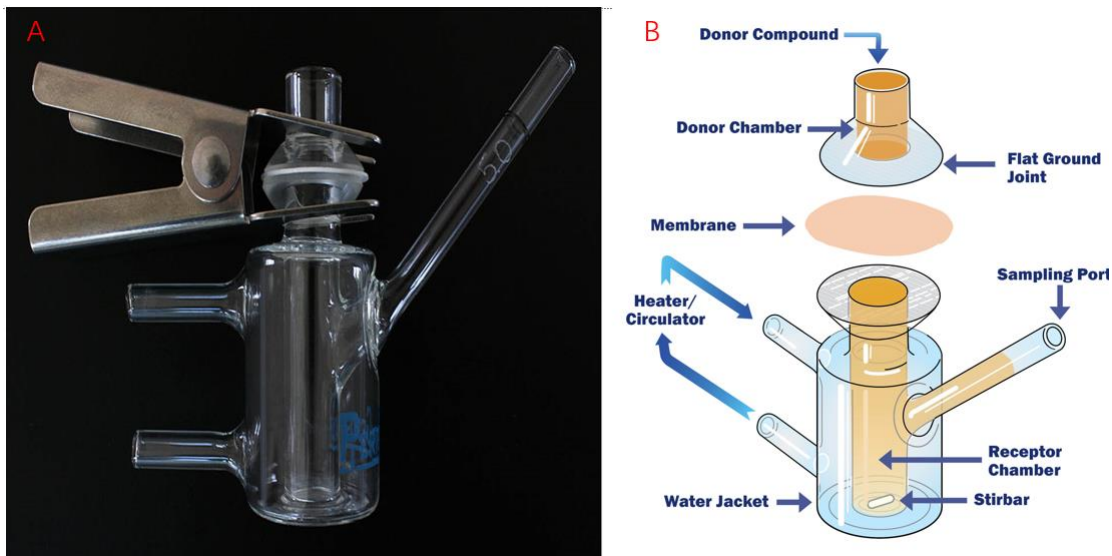


Figure 17 (A) The photo of Franz cell; (B) an oblique view of a jacketed Franz cell with a flat ground joint [1]

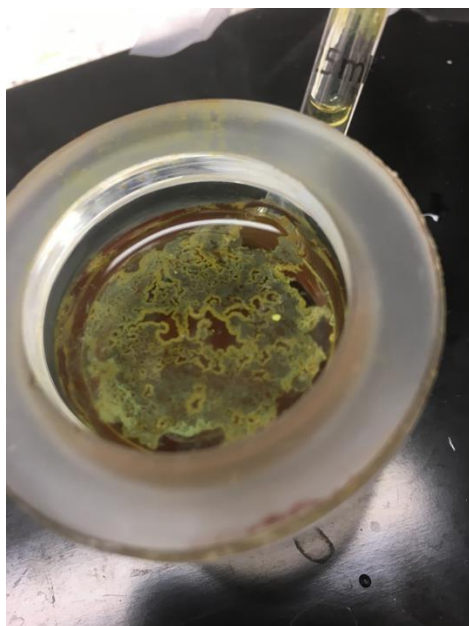


Figure 18 Photo of TAPB-PDA membrane synthesized in Franz cell

2.6 References

- [1] Chong, Jonathan H., et al. "Highly stable keto-enamine salicylideneanilines." *Organic letters* 5.21 (2003): 3823-3826.
- [2] Mehr, S. Hessam M., et al. "Formylation of phenols using formamidinium acetate." *Organic & biomolecular chemistry* 15.3 (2017): 581-583.
- [3] Kandambeth, Sharath, et al. "Construction of crystalline 2D covalent organic frameworks with remarkable chemical (acid/base) stability via a combined reversible and irreversible route." *Journal of the American Chemical Society* 134.48 (2012): 19524-19527.
- [4] Kaleeswaran, D., Pratap Vishnoi, and Ramaswamy Murugavel. "[3+ 3] Imine and β -ketoenamine tethered fluorescent covalent-organic frameworks for CO₂ uptake and nitroaromatic sensing." *Journal of Materials Chemistry C* 3.27 (2015): 7159-7171.
- [5] Wang, Liangying, et al. "Fluorene-Based Two-Dimensional Covalent Organic Framework with Thermoelectric Properties through Doping." *ACS applied materials & interfaces* 9.8 (2017): 7108-7114.
- [6] Dey, Kaushik, et al. "Selective molecular separation by interfacially crystallized covalent organic framework thin films." *Journal of the American Chemical Society* 139.37 (2017): 13083-13091.
- [7] Matsumoto, Michio, et al. "Rapid, low temperature formation of imine-linked covalent organic frameworks catalyzed by metal triflates." *Journal of the American Chemical Society* 139.14 (2017): 4999-5002.
- [8] Matsumoto, Michio, et al. "Lewis-Acid-Catalyzed Interfacial Polymerization of Covalent Organic Framework Films." *Chem* 4.2 (2018): 308-317.
- [9] Ribeiro, Ana CF, et al. "Diffusion of sodium alginate in aqueous solutions at T= 298.15 K." *The Journal of Chemical Thermodynamics* 74 (2014): 263-268.
- [10] Rodríguez-San-Miguel, David, et al. "Crystalline fibres of a covalent organic framework through bottom-up microfluidic synthesis." *Chemical Communications* 52.59 (2016): 9212-9215.
- [11] Thote, Jayshri, et al. "Constructing covalent organic frameworks in water via dynamic covalent bonding." *IUCrJ* 3.6 (2016): 402-407.
- [12] Franz Cell, <http://permeagear.com/parts-of-a-franz-cell/>

3 Results and Discussions

3.1 General methods

The X-ray diffraction patterns of the samples were measured using a Rigaku Ultima IV X-ray Diffractometer with Cu K α radiation ($\lambda = 1.54 \text{ \AA}$) at a scanning rate of 10 °C/min, with accelerating voltage and current of 40 kV and 20 mA, respectively. Film samples were grinded into powder prior to analysis. Data was collected using a 0.05° 2 θ step scan from 1-30° with an exposure time of 2 sec per step.

FT-IR spectra were measured with the use of Thermo Scientific Nicolet 6700 Fourier transform infrared (FT-IR) spectrometer.

IV measurement was taken with the use of Alessi REL-4800 probe station at room temperature.

Brunauer–Emmett–Teller (BET) surface areas measurements were performed on a Micromeritics Tristar II 3020 surface area and pore size analyzer. Samples were degassed and activated at 250 °C under the protection of nitrogen for more than 12 hours.

Scanning electron microscopy (SEM) was performed by an FEI Quanta-600 FEG Environmental SEM with 5-15 kV accelerating voltage.

¹H NMR spectra were recorded in deuterated solvents on a BURKER AVANCE III ULTRA SHIELD PLUS 800MHZ. Chemical shifts are reported in parts per million (ppm, δ) using the solvent as internal standard. ¹³C NMR spectra were recorded on the same instrument using the solvent as an internal standard.

3.2 Characterization of COF-TpFn

The crystallinity of COF-TpFn was measured by powder X-ray diffraction (PXRD) analysis. The fig. 19 shows the PXRD pattern of the as-synthesized COF-TpFn. The intense first diffraction

peak appears at 2θ of 3.54° which correspond to the (100) plane reflection. By the Bragg's law equation,

$$\lambda = 2d\sin\theta$$

the porous diameter of COF-TpFn structure is calculated as 24.9 Å.

$$d = \frac{\lambda}{2\sin\theta} = \frac{1.54 \text{ \AA}}{2 \cdot \sin(1.77^\circ)} = 24.9 \text{ \AA}$$

The wide peak with 2θ of 26.1° is assigned as the (001) plane. Calculating the d-spacing between (001) planes, the π - π stacking distance between the successive COF layers is found to be 3.41 Å.

$$d = \frac{\lambda}{2\sin\theta} = \frac{1.54 \text{ \AA}}{2 \cdot \sin(13.05^\circ)} = 3.41 \text{ \AA}$$

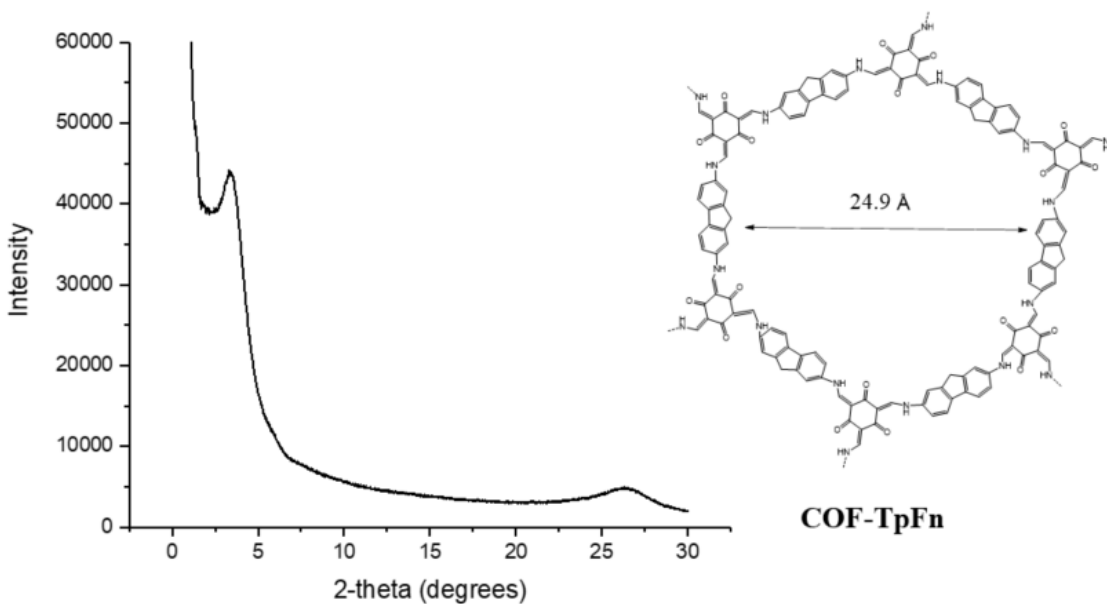


Figure 19 PXRD pattern and structure of COF-TpFn

The FT-IR spectra shown in fig. 20 revealed the disappearance of the N-H stretching frequency at $3100\text{--}3300 \text{ cm}^{-1}$ corresponding to the free diamines. The carbonyl stretching frequency at 1560 cm^{-1} indicated the aldehyde carbonyl -C=O bonds. What is more, the appearance of peaks at 1250 cm^{-1} corresponding to the stretching of the -C=C- and -C-N- bonds confirmed the successful formation of COFs.

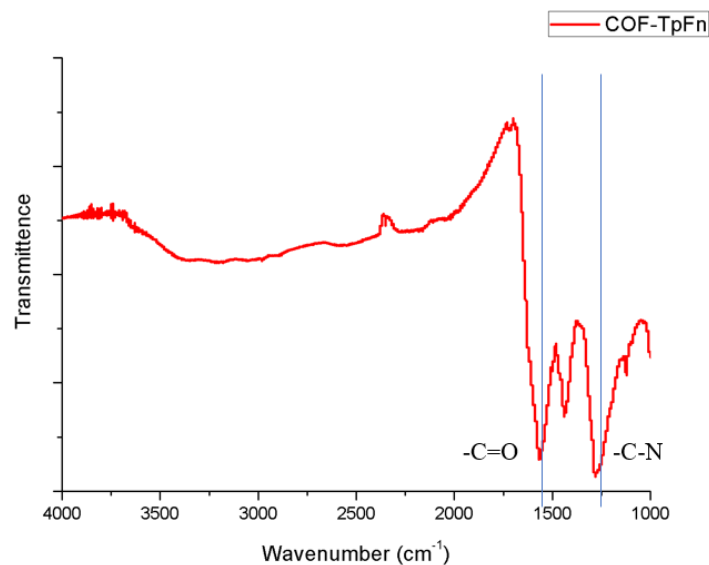


Figure 20 Infrared spectra of TpFn COF

TpFn was synthesized via an improved solvothermal method. First, the solvents used in this experiment were *o*-DCB and DMAC instead of mesitylene and dioxane. Moreover, the vigorous stirring in the solution promoted the mixing of precursors in the solvents. Last, a balloon filled with inert gas was used for degassing the reaction system to replace the complicated freeze-pump-thaw set-up in the conventional synthesis. Fig. 21 shows the PXRD patterns of TpFn via three different ways. Obviously, the product made from the improved solvothermal method presents the most efficient result with obvious diffraction peaks. Conventionally synthesized TpFn shows inconspicuous peaks, and no evidence of crystallinity is observed in the TpFn synthesized through the water-based route.

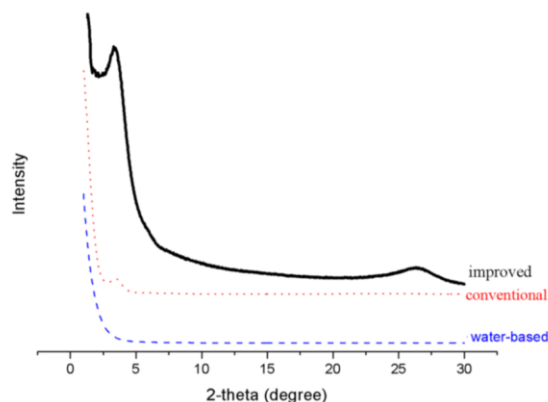


Figure 21 PXRD of TpFn synthesized via improved solvothermal method (black solid); conventional solvothermal method (red dot); and water-based hydrothermal method (blue, dash)

The porosity of product can also be confirmed through the BET measurement. The improved solvothermal synthesized TpFn shows a surface area of $850.7 \text{ m}^2 \text{ g}^{-1}$, which is much higher than that synthesized using the conventional solvothermal (BET: $328.7 \text{ m}^2 \text{ g}^{-1}$) and water-based hydrothermal (BET: $108.3 \text{ m}^2 \text{ g}^{-1}$). Hence, the improved solvothermal synthesized TpFn exhibits higher crystallinity and better porous structure compared with the COF synthesized via other traditional methods.

Table 2 Surface areas of TpFn synthesized via different methods

Synthesis method	Surface Area ($\text{m}^2 \text{ g}^{-1}$)
Improved solvothermal	850.7199
Conventional solvothermal	328.6872
Water-based route	108.3196

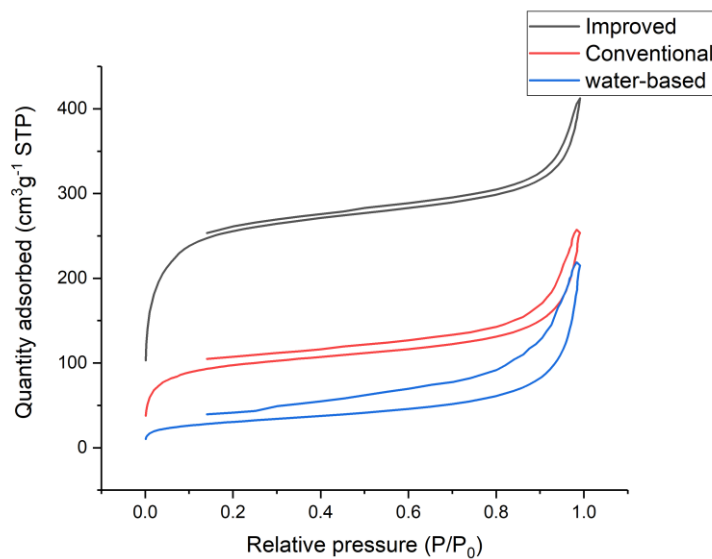


Figure 22 N_2 adsorption isotherms of TpFn synthesized using the improved solvothermal (black), the conventional (red) and water-based (blue) route.

3.3 Characterization of TAPB-TFP

The two similar PXRD patterns of the TAPB-TFP powder synthesized via solvothermal method and membrane via interfacial polymerization are shown in fig. 23 A. Peaks at 2θ of 5.88° correspond to the (100) plane reflection and the wide peaks with 2θ of 24.2° refer to the (001) plane. By the same method, the porous diameter of TAPB-TFP is 15.0 \AA and the π - π stacking distance between the adjacent COF layers is calculated to be 3.67 \AA .

Fig. 23 B revealed that COF membrane and powder had the accordant FT-IR spectra in which the peak that appeared at 1619 cm^{-1} indicated the C=O stretching frequencies, and the presence of peaks around 1300 cm^{-1} was due to the C-N bonds.

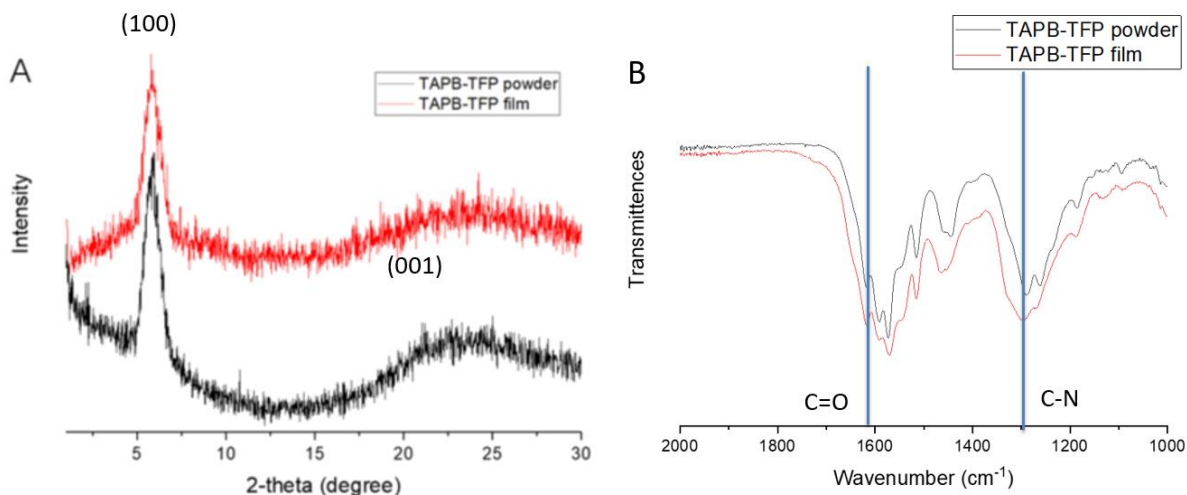


Figure 23 (A) PXRD of TAPB-TFP powder (black) and film (red); (B) FTIR spectra of TAPB-TFP film (red) and powder (black)

3.4 Characterization of TAPB-TFB membrane

The PXRD pattern of the TAPB-TFB film synthesized via interfacial method exhibits peak at 2θ of 5.88° corresponding to the (100) plane reflection, and the wide peaks with 2θ of 24.2° refer to the (001) plane. By the same method, the porous diameter of TAPB-TFB is 15.0 \AA and the π - π stacking distance between the adjacent COF layers is calculated to be 3.67 \AA .

Fig. 24 B revealed that TAPB-TFB membrane and powder had the accordant FT-IR spectra where the C=N stretching frequencies appear at 1622 cm^{-1} and the presence of peaks around 1690 cm^{-1} is due to the C=O bonds.

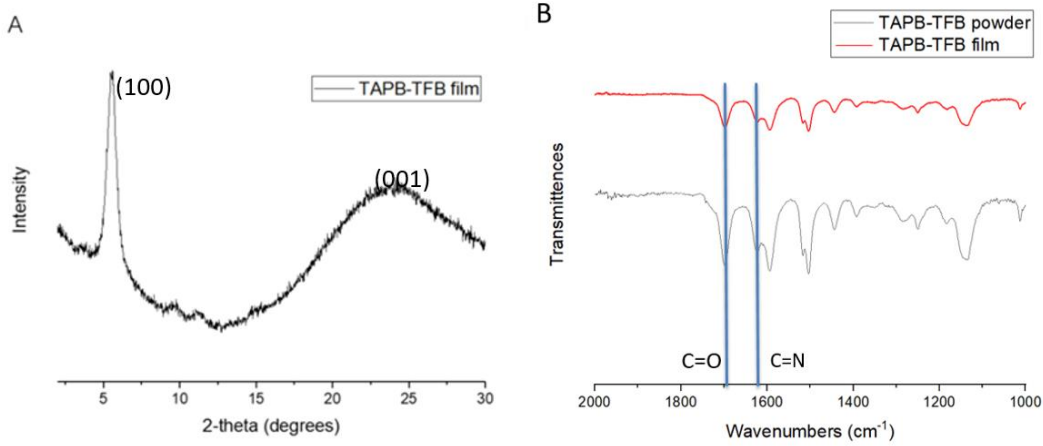


Figure 24 (A) PXRD of TAPB-TFB film; (B) FTIR spectra of TAPB-TFB film (red) and powder (black)

3.5 IV measurement of iodine doped COFs

The current voltage measurements are shown in fig 25. Both of two results exhibit good linearity between current and voltage and the resistance can be estimated by the reciprocal of slope. For TpFn, the resistance at room temperature is:

$$R_{\text{TpFn}} = \frac{1}{7 \times 10^{-13}} = 14.2 \times 10^{12} \Omega$$

After doping with iodine, the resistance is decreased to:

$$R_{\text{I}_2@\text{TpFn}} = \frac{1}{6 \times 10^{-9}} = 16.7 \times 10^8 \Omega$$

Since the two pellets are in the same shape, a conclusion can be obtained that the compressed pellet of $\text{I}_2@\text{TpFn}$ exhibited an improved conductivity with increasing about 10,000 times after doping with iodine.

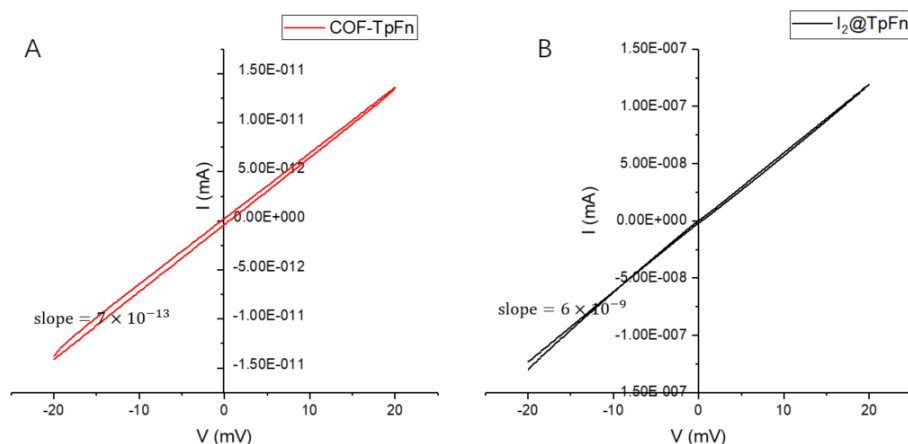


Figure 25 Current-voltage measurement of COF-TpFn (A) and I₂@ TpFn (B)

3.6 Characterization of TAPB-PDA membrane

Characterization by FTIR revealed a peak at 1680 cm^{-1} corresponding to the aldehyde stretch and a peak at 1620 cm^{-1} corresponding to C=N bonds to confirm the formation of COFs structure (Fig. 26).

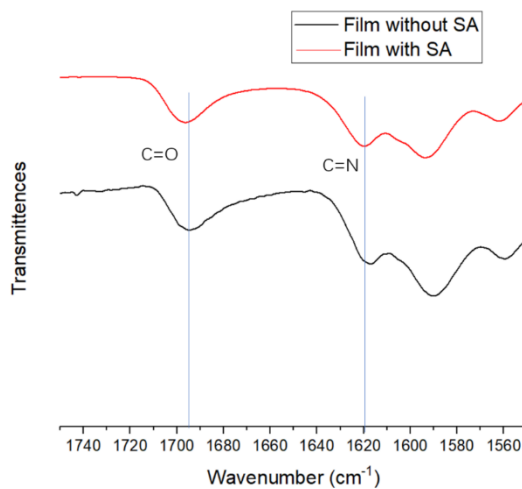


Figure 26. Infrared spectra of TAPB-PDA membrane

The x-ray diffraction patterns obtained from both interfacial synthesis strategy exhibited the main peak at 2.88° corresponding to the (100) plane reflection, which matched well to the

pattern observed in the TAPB-PDA powder synthesized via the solvothermal method. The PXRD pattern of TAPB-PDA membrane is not as obvious as that of powder sample because the activation procedure using supercritical CO₂ was not operated for membrane samples.

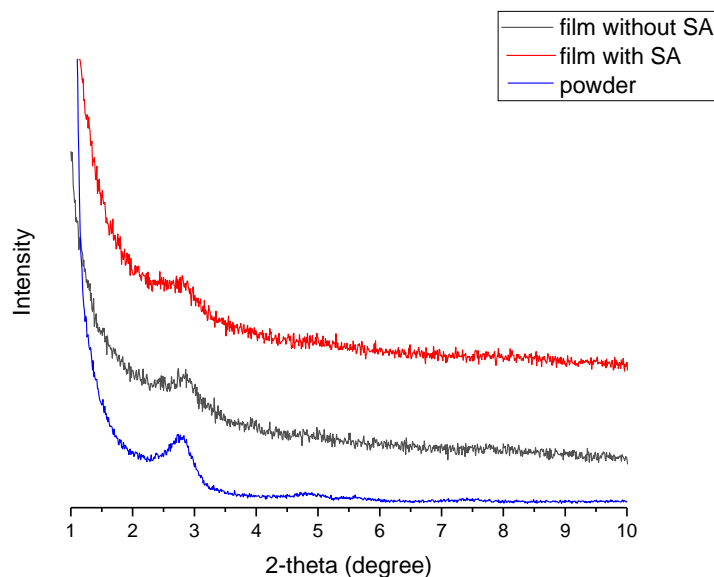


Figure 27 PXRD patterns of TAPB-PDA films synthesized with sodium alginate (red) and without sodium alginate (black) and TAPB-PDA powder synthesized via solvothermal route (blue)

The scanning electron microscopy (SEM) was exploited to characterize TAPB-PDA thin films. For the film formed without sodium alginate in the spacer layer which was shown in Fig 28 A, the SEM images reveal a morphology of spherical particles about 1 μ m in diameter aggregates to form an interval thin film. In contrast, the micrographs shown in Fig 29 A exhibited a more uniform film, which confirm that sodium alginate in the spacer layer could control the diffusion to make the film smoother.

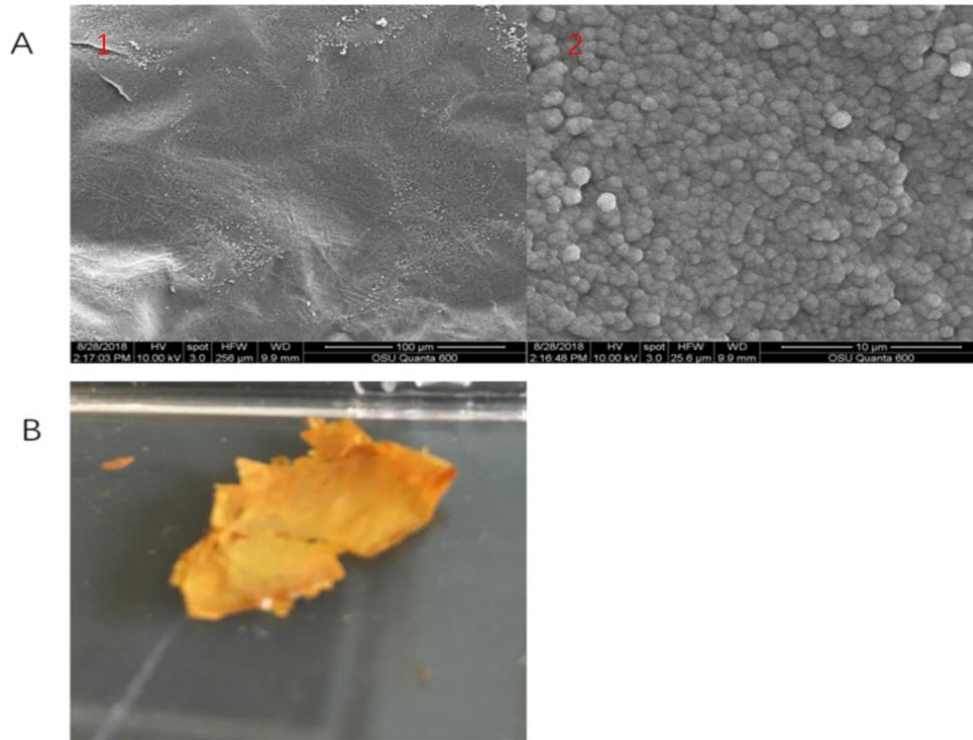


Figure 28 (A) SEM images of TAPB-PDA membrane at different magnifications and (B) photo of TAPB-PDA membrane

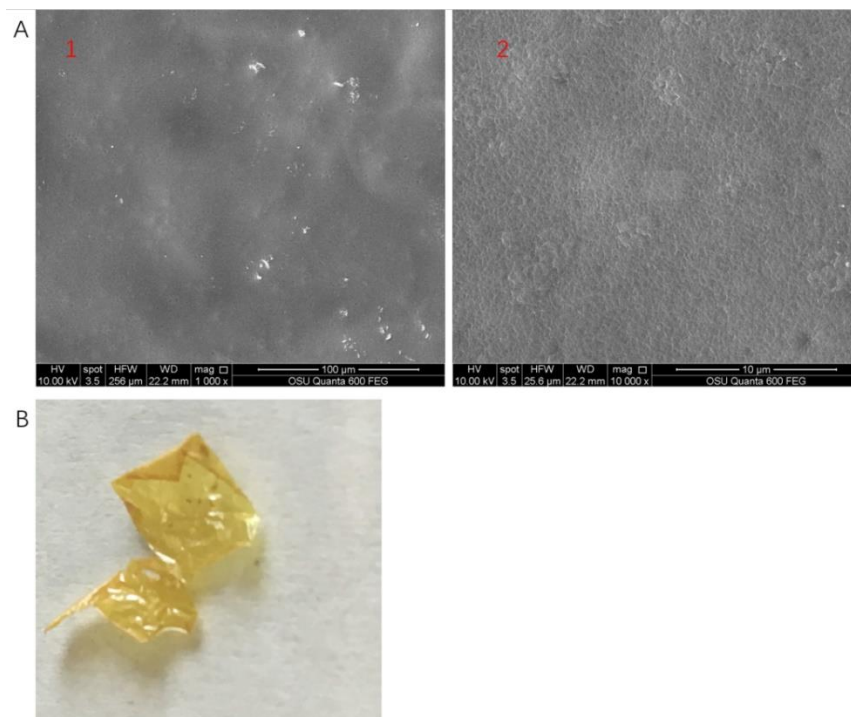


Figure 29 (A) SEM images of TAPB-PDA membrane synthesized by introducing sodium alginate in spacer layer and (B) photo of TAPB-PDA membrane

The TAPB-PDA synthesized via the interfacial method exhibited a BET surface area of $277.8 \text{ m}^2/\text{g}$, which confirms the porosity of COFs.

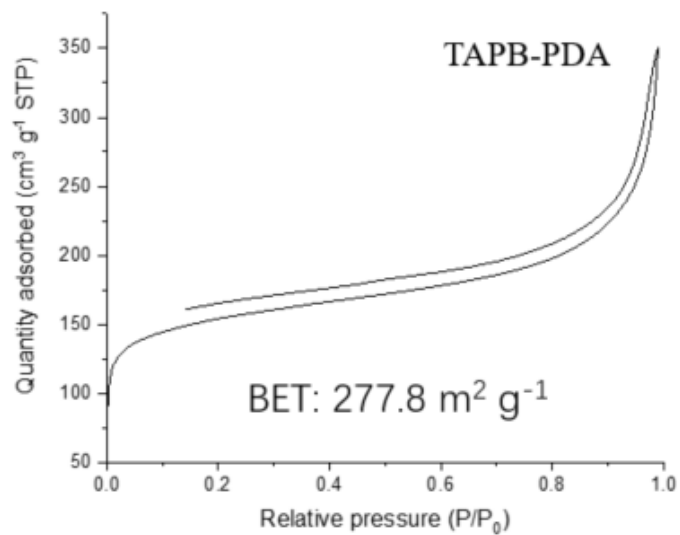


Figure 30 N₂ adsorption isotherms of TAPB-P

4. Conclusion and Future Works

4.1 Conclusion

COF-TpFn was synthesized via the revised solvothermal method in which nitrogen filled balloon and stirring bar are used in the reaction system to synthesize COFs with higher crystallinity and surface areas. The revised method is facile to operate compared with the conventional solvothermal synthesis.

Two kinds of COFs TAPB-TFP and TAPB-TFB were synthesized via the interfacial polymerization, and TAPB-PDA was interfacially synthesized by using m-cresol as organic phase instead of aggressive 1,4-dioxane and mesitylene.

Several techniques such as X-ray diffraction (XRD), scanning electron microscope (SEM), Fourier transform infrared (FTIR) spectroscopy and the nitrogen sorption isotherm analysis were performed to characterize COFs synthesized in the experiments. This work provides a facile and safe strategy to fabricate COFs membrane under ambient conditions. The free-standing membrane can be transferred onto other substrates to explore their potential applications in filtering large molecules in the future.

4.2 Future work

In the future, a more suitable measurement needs to be found or designed to characterize the electric properties of iodine doped TpFn and COFs membranes including the measurement of conductivity and Seebeck coefficient. Moreover, the molecular separation performance will be evaluated by transferring synthesized COFs membrane onto the substrate. More suitable membrane should be found to use to control diffusion, and the procedure of interfacial synthesis in Franz cell requires revision to make uniform thin film.

Appendix: ^1H and ^{13}C NMRs for Synthesized Compounds

